Acceleration-Based Learning of Pitch Misalignment in Wind Turbine Blades

Journal of Physics: Conference Series **3224** (2026) 062002 doi:10.1088/1742-6596/3224/6/062002

Acceleration-Based Learning of Pitch Misalignment in Wind Turbine Blades

Sabrina Milani[1], Jessica Leoni[1], Stefano Cacciola [2], Alessandro Croce [2] and Mara Tanelli [1]

[1] Dipartimento di Elettronica, Informazione e Bioingegneria (DEIB), Politecnico di Milano, Piazza L. Da Vinci 32, Milan, 20133, Italy

[2] Dipartimento di Scienze e Tecnologie Aerospaziali (DAER), Politecnico di Milano, Politecnico di Milano, Via La Masa, 34, Milan 20156, Italy

E-mail: sabrina.milani@polimi.it

Abstract. Effective monitoring of wind turbine operations is crucial to ensure efficiency and to reduce downtime, particularly considering offshore and remote installations. Our previous studies considered automatic pitch misalignment detection using signals from mechanical moment sensors, which are expensive and may not be available in all real-world turbines. To provide a cost-effective and more applicable solution, this paper builds upon the previously proposed method aiming to achieve comparably good performance by relying on signals measured by acceleration signals, collected from a set of triaxial accelerometers placed on the fixed reference frame of the turbine. For the learning phase, we employ features based on the physical behaviour of the system with a specific focus on integrating frequency-domain information. Also, to face the restricted set of available signals, an additional layer is introduced to localize the anomaly. The results confirm the validity of the method even when used with this reduced set of signals, thus broadening the potential for the model to be applied in more widespread scenarios.

1. Introduction

Persistent vibrations from a misaligned rotor in wind turbines can significantly affect the lifespan and efficiency of these systems, leading to mechanical failures in key components like gearboxes, electronic boards, sensors, motors, and blades. This can reduce energy production and requires frequent inspections of actuators, which, particularly for offshore or remote turbines, can be costly and challenging. To improve efficiency, a shift towards condition-based maintenance is crucial. This requires an automatic diagnostics algorithm for ongoing health monitoring, early fault detection, and timely repairs to prevent major damage. Detecting pitch misalignment in wind turbines has been approached in the literature through two main methods: physics-based models and machine learning techniques. Physics-based models, as discussed by [1] and [2], require a physical model of the system to identify anomalies rotor imbalances. These methods often require a tailored representation of the system, which, while ensuring interpretability and an accurate description of its behavior, also increases complexity and limits their applicability to real wind turbine systems. Additionally, they typically rely on signals that are difficult to obtain in real-world systems, and lack accuracy and robustness in turbulent wind conditions, which are common in actual wind turbine operations. Other model-based techniques have been proposed

in [3–6], where the focus is to detect the presence of rotor imbalances and target them through a load compensation technique or via suitable control actions. These techniques, though, do not propose a method to specifically localize the anomaly or require a modification of the turbine control system, a task practically unfeasible in the case of existing turbines equipped with a certified controller.
On the other hand, machine learning methods, such as those proposed by [7], provide high generality and require reduced design time. However, while they can detect pitch misalignment, localization of the anomaly and estimation of its severity remain a challenging operation. In addition, advanced approaches, like those based on deep learning [2], lack interpretability, making it difficult to understand the decision-making process, which is crucial for promoting their adoption. Recent studies show that interpretable models can enhance the understanding of anomaly detection processes, as the approach we proposed in our prior work [8, 9]. Indeed, the framework can improve system reliability and efficiency while operating in turbulent wind conditions without interfering with the turbine's nominal operation.
In our prior works, [8, 9], we designed a machine-learning based diagnostic framework to detect the pitch misalignment in wind turbines system. However, that approach is based on the mechanical moments, that in some industrial applications may be too costly or not-available measurements. Therefore, in this work we evaluate the effectiveness and robustness of the proposed method when considering even a more accessible and less cost-demanding set of sensors, namely accelerations on the fixed reference frame of the turbine and specifically located in the tower top. In a similar way as in the previous works, the extraction of the relevant features is performed in a real-time fashion considering physics-based features in the frequency domain within a fixed number of rotor revolutions to avoid dependency on the rotor velocity. According to the designed framework, if any misalignment is detected, this is then classified as low, medium or high according to the detected degree of misalignment by the first classification layer. Then, in case of an anomalous behaviour of the rotor, the second layer of the original framework architecture localizes the anomaly on the affected blade. Results of this procedure applied to a different set of signals still is capable of achieving satisfactory performance, even under turbulent wind conditions, though the noisier and less sophisticated nature of employed signals.

2. Preliminary Analysis

This section provides insights into the simulation environment and dataset, which is the same as that used in our prior study. The dataset, composed of several 600-second simulations, comes from a virtual generator, consisting of a reference 5 MW wind turbine [10] implemented in the software `Cp-Lambda` (a Code for Performance, Loads, Aeroelasticity by Multi-Body Dynamics Analysis) a state-of-the-art general-purpose multibody simulator [11]. The model is characterized by flexible tower, blades, and shaft, whereas the blade element momentum theory is used for modeling rotor aerodynamics, including hub- and tip-losses and tower shadow. To measure relevant signals, the turbine model is also equipped with virtual sensors. All simulations were conducted in different pitch misalignment conditions, individually imposed on the three blades and turbulent inflow that was defined according to the Standards [12] (Normal Turbulence Model). In addition, the simulations are conducted with an air density set at $\rho = 1.225\ kg/m^3$ and, the examined wind speeds span a range from $v = 5\ m/s$ to $v = 25\ m/s$, with the wind direction aligned with respect to the rotor, meaning with zero mean yaw misalignment. Multiple simultaneous offsets are not part of this work, and the full list of DLC1.1 ([12]) simulations (from cut-in to cut-out speed), was repeated 50 times, for different pitch misalignments, changing every time the turbulence seed. The key characteristics for the conducted simulations can

be summarized as follows: simulations are conducted with air density equal to $\rho = 1.225\ kg/m^3$, turbulence type NTM and class A with a wind speed varying from $v = 5m/s$ to $v = 25m/s$ and null rotor ywa misalignment. More in detail, 24 sets of simulations were dedicated to blade 1 misaligned, 10 sets for blade 2 and 3, and 6 sets for the balanced scenario, *i.e.,* without misalignment. The maximum entity for the considered pitch offset is 2.0 deg, while the minimum one is equal to 0.5 deg.

3. Preliminary Analysis and Features Engineering

In this section, the behaviour of the wind turbine under healthy and anomalous conditions with respect to the available set of signals is analyzed. By discussing the comparison between the theoretical and experimental behavior of the system provides a comprehensive physical understanding of the rationale behind the choice of the features extracted from the accelerations signals to detect and localize the fault when present. The idea is to stress the relevance of each feature in meaningful patterns that highlight a physical relevance with respect to a specific monitoring conditions of the turbine.

3.1. Signals Processing and Exploratory Analysis

According to physics, in a balanced rotor loads are transmitted to the fixed frame at harmonics multiple of the number N_B of blades only (in the case under study, $N_B = 3$). Conversely, unbalanced rotors transmit loads at all harmonics, with the $1 \times Rev$ frequency being the most energetic and deceptive one. This holds true also for the accelerations signals. The indicators in this case highlighting the existence of the $1 \times$ Rev harmonic contribution in a misaligned scenario are the Accelerations along the lateral and vertical axes A_y and the top-down acceleration A_z. Given the less precise nature of acceleration signals, this holds true for a reduced range of velocities, in particular starting from a wind velocity of $v = 11m/s$. For lower wind speeds, there is no sufficient differentiability in the data for a precise classification. When a blade is misaligned, a change in in the amplitude of the $1\times$ Rev harmonic conveyed to the fixed reference frame is observed, providing insights into the severity of the misalignment through its amplitude. Despite deviating from exact periodicity due to turbulent wind conditions, with a sufficiently long time window analysis, turbulence effects tend to compensate and balance, revealing only minor $1\times$ Rev harmonic contributions in a healthy balanced rotor. Hence, the presence of the $1\times$ Rev harmonic in the frequency response of these signals clearly indicates misalignment of one of the blades while the amplitude of the peak shows a dependency on the severity of the anomaly. In the frequency response of these signals measured in the tower top position, another contribution can be seen in the frequency response placed around $1.5\times$ Rev harmonic. This represents the contribution of the tower natural frequency.

When considering different wind speeds, the peak position is shifted along the spectra frequencies also in case of accelerations. To remove this dependency, the Fourier Transformations applied on tower top accelerations are performed with respect to the Azimuth signal. In such a way, the harmonic response depends on the rotor frequency revolutions only remaining at the $1 \times$ Rev harmonics, regardless of wind speed. Figure 1 illustrates azimuth-based power spectra at a medium wind speed of $v = 15m/s$ for the Acceleration along z direction in a healthy case and two anomalous cases (0.5 deg and 1.5 deg misalignment, respectively). As previously mentioned, regardless the condition of the rotor (healthy or anomalous) all cases exhibit a peak of different amplitude placed around $1.5\times$ Rev harmonic, which represents the contribution of the tower frequency. Conversely, for the anomalous cases the peak at the $1\times$ Rev harmonic confirms the presence of the anomaly, while the healthy case lacks a peak at $1 \times$ Rev. The same pattern is observed in the Acceleration along y direction for the same wind speed range. Therefore, in

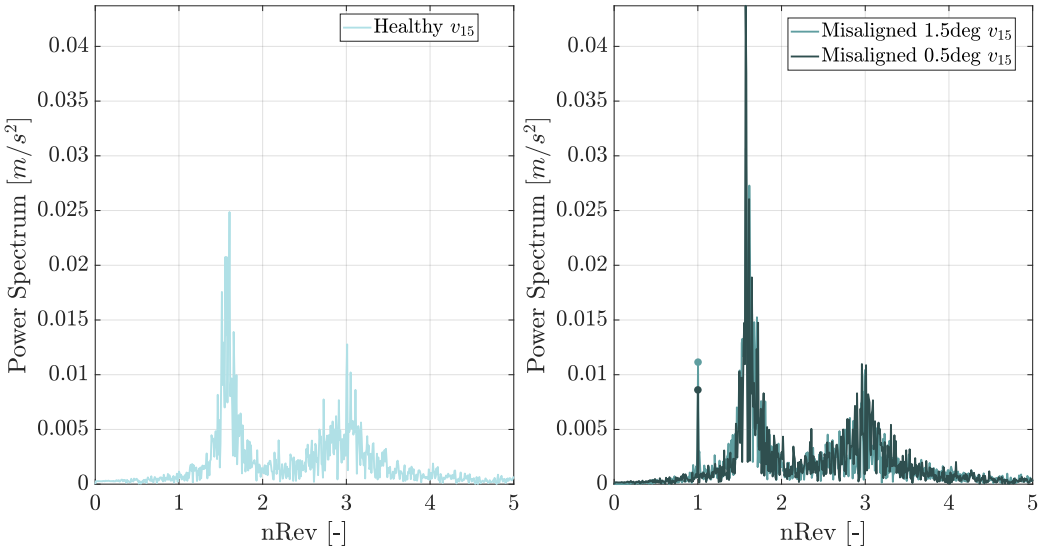

Figure 1. Acceleration spectra for a healthy (on the left) and two different misaligned cases (on the right) all at speed of 15 m/s

.

this context, the crucial factor for distinguishing between the healthy and expected behaviour, characterized by a minimal peak amplitude, and the anomalous rotor conditions, characterized by an increase in peak amplitude, is once again the area subtended the peak at the 1 × Rev harmonics or similarly the value of the amplitude of the peak at the 1 × Rev harmonics.
In addition, since the available measurements come from the fixed reference frame, the features extracted in our previous work cannot be exploited in this case. Therefore, we investigate additional features, which were considered only partially in our previous study, where the momenta module analysis was enough to effectively detect the misalignment and locate it. To this end, we rely on the physical knowledge that, whenever a blade is affected by pitch misalignment, the contribution is seen both in the amplitude of the 1 × Rev harmonic at the fixed reference frame and information related to the affected blade can be derived by its phase. The acceleration along y direction of the generic i_{th} blade can be expanded in Fourier series as:

$$A_i = A_{0,i} + \sum_{n=1}^{\infty} (A_{nci} \cdot cos(n\psi_i) + A_{nsi} \cdot sin(n\psi_i)) \tag{1}$$

where, $A_{0,i}$ is the 0th harmonic (a constant term), representing the mean of the acceleration for the i_{th} blade, n represents the harmonic order, where each harmonic describes oscillations at a different multiple of the fundamental frequency of rotation, A_{nci} and A_{nsi} represent the cosine and sine coefficients for the n-th harmonic of the acceleration for the i-th blade, ψ_i is the azimuthal angle for the i-th blade. The phase ϕ_i of a generic harmonic component can be computed from the sine and cosine coefficients as follows :

$$\phi_i = atan(A_{nsi}, A_{nci}) \tag{2}$$

Figure 2 reports the 2-D features space for the phases of the 1 × Rev harmonic lateral and top-down accelerations. Although phases of these components are represented in the plot as more sparse in the 2-D features space than in the case of mechanical moments, phases can still be grouped according to the affected blade and to the sign of the misalignment as well.

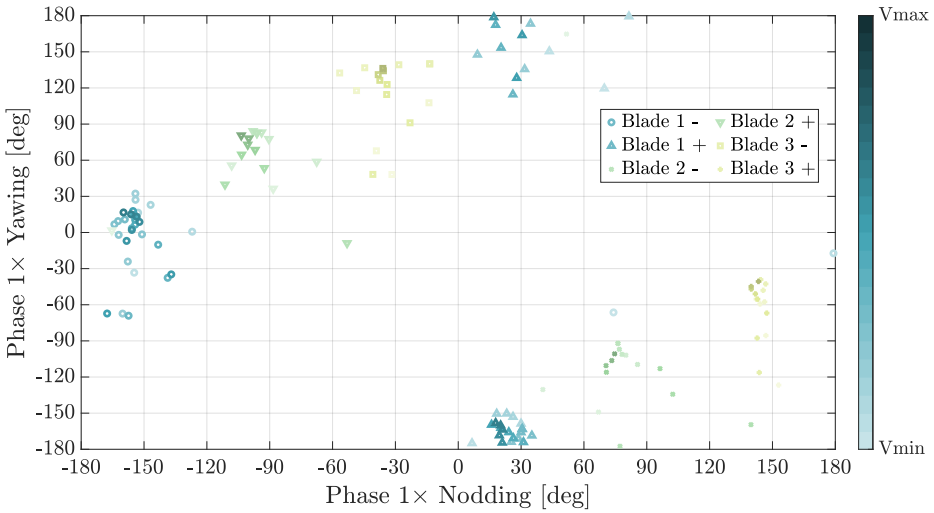

Figure 2. Accelerations 1 × Rev harmonics phases. Each instance in which the same blade is misaligned is represented with the same color, while a different marker within the same color represents a different misalignment sign for the same blade. Different instances of the same symbol and color, with shades varying from a lighter to a darker tone represent different wind velocities for the same came. Specifically, the wind velocity increases from the minimum to the maximum considered speed v_{min} = 11m/s - v_{max} = 25m/s as the bar on the right reports. The bar is only reported for the case in which blade 1 is misaligned, the same meaning holds for the other cases and colors.

.

3.2. Features Extraction

As outlined in our previous research, we aim to develop an interpretable machine learning framework. To achieve this, we focused solely on extracting physics-based features, which would a posteriori help us in understanding the decision-making process adopted by the classifier. To identify the most influential set of physics-based features, we initially extracted a broad range of indicators that could potentially be relevant from a physical perspective. Therefore given that 1 × Rev harmonics plays a crucial role both in detecting the presence of the anomaly and in locating the affected blades, we have identified the following features:

- area subtended the peak at the 1 × Rev harmonics from the Accelerations along Y and Z direction
- the amplitude of the peak at the 1 × Rev harmonics
- the phase of these components

These frequency-domain features are extracted using a moving window approach, as in the original framework, to ensure that the classification algorithm's predictions are generated in real-time. This approach allows for focusing on the behavior of the scenario within a specified number N of rotor revolutions, regardless of the time required to complete them. Given the duration of the simulations (each lasting 600 seconds) and the range of wind velocities, a window of 40 azimuth revolutions has been adopted. This window size ensures a robust Fourier transform and effectiveness across different wind velocities. According to this procedure, each window is transformed into a two-dimensional instance, characterized by either the acceleration spectrum area or the peak. Overall, there are 88 instances for healthy cases, 121 for lower misalignment, 210 for medium misalignment, and 37 for higher misalignment degrees.

Classification Report				
Label	**Precision**	**Recall**	**F1-score**	**Support**
Healthy	0.88	0.93	0.91	88
Low	0.82	0.83	0.82	121
Medium	0.89	0.92	0.91	210
High	0.96	0.62	0.75	37

Table 1. Metrics computed from the fault and quantification output considering spectra area features

4. Severity Assessment and Method

Once feature extraction has been performed, each window corresponds to a point in a 2D space. The coordinates of this point are determined by the area subtended the peak at the 1 × Rev harmonics or by the amplitude of the peak at the 1 × Rev harmonics from the lateral and top-down Accelerations within that window. All these instances derived from this process are exploited for training and evaluating the performance of a *Random Forest Classifier*. This classifier is instrumental in discerning the presence of misalignment, quantifying its severity, and locating the misaligned blade as well as indicating the sign of the misalignment. The Random Forest algorithm, which we have selected for its interpretability and robustness, is one the most explainable state-of-the-art bagged tree-based classification methods [13]. This approach combines the outcomes of numerous binary decision trees, which split the data in an iterative way based on specific criteria, reducing variations within the identified clusters at each step. The splitting process is carried out considering specific criteria, including accuracy, precision, and the Gini index [14]. For the severity assessment, each instance is labeled based on the degree of misalignment while for the localization assessment the label to predict was the misaligned blade. In more detail, the classifier is trained to recognize in the first assessment layer, four classes of Pitch Misalignment (PM): *0 deg PM* for healthy cases; $0.5\ deg \leq p < 1.0\ deg\ PM$ for low misalignment; $1.0\ deg \leq p < 1.5\ deg\ PM$ for medium misalignment; $p \geq 1.5\ PM$ for large misalignment, where p represents the actual value of the detected misalignment. Moreover, this model was composed of 5 trees, each with depth 3. While, in the second localization layer, that is engaged whenever a misalignment is detected, six classes are expected, namely two for each blades according to a positive or a negative misalignment and in this case the model was composed of 4 trees, each with depth 3. The parameters of the classificators have been chosen as a trade off between accuracy and computational time, which is increasing with the depth of each instance of a tree. Regardless the algorithm layer, the data is split according to a balanced fashion into 70.0% for training and 30.0% for testing in a stratified manner; additionally, 10-fold cross-validation is applied, and the average performance across all folds is reported.

5. Results and Discussion

Average results for evaluation metrics when the algorithm is tested on the set of features including the area subtended the peak at the 1 × Rev, including precision, recall, F1-Score, and support are reported in Table 1. These metrics have been chosen for their relevance in evaluating the performance of anomaly detection techniques. Precision is a key metric that measures the accuracy of predictions by evaluating the ratio of correctly predicted instances to the total predicted instances for a given class. In contrast, recall (or sensitivity) assesses the accuracy of predictions for a class relative to all actual instances of that class. The F1-Score combines

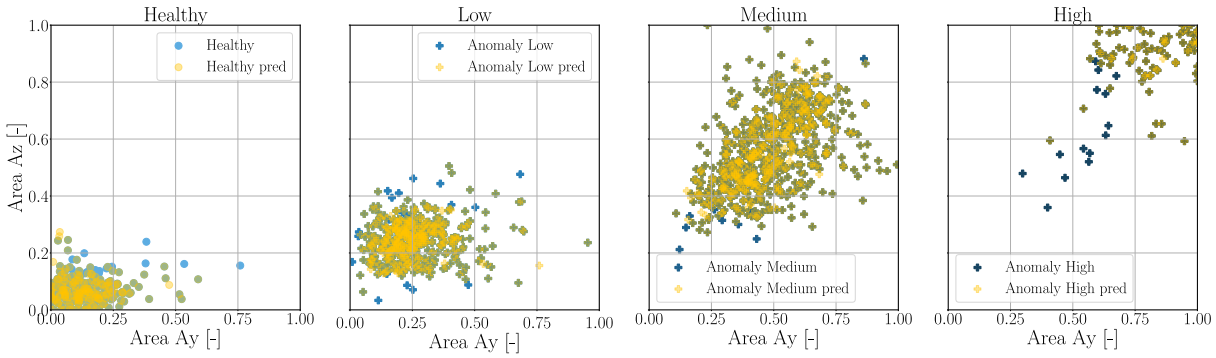

Figure 3. Misalignment Severity Assessment Results. This Figure shows a comparison of predicted misalignment severity (in yellow) with the actual one, demonstrating consistency across severity levels.

both precision and recall, representing their harmonic mean. Finally, support indicates the frequency of each label within the class being considered. By considering F1-Score as a metric, our approach proved effective at detecting the presence of misalignment and further classifying its severity class, with an average F1-Score of 88.0% regardless of the turbulence intensity and with a wind speed ranging from 11 to 25 m/s, with respect to an average F1-Score of 93.5% in the case of mechanical moments.

Delving into specifics, our framework exhibits a good F1-Score performance, achieving 88.0% accuracy in detecting the healthy class, 82.0% for the low, 91.0% for the medium, and 75.0% for the high misalignment class, while in the case of mechanical moments the method achieved 95.0% accuracy in detecting the healthy class, 93.0% for the low, 94.0% for the medium, and 90.0% for the high misalignment class. Indeed, these achievements stand out as slightly less remarkable with respect to the case study in which mechanical moments are considered. Accelerations, as previously mentioned show a more noisy behaviour and tend to be less accurate when considering low wind velocities. Nevertheless, diverse and challenging operating conditions are still considered in our experiments, including turbulent scenarios and strong winds. Notably, our approach still is capable of identifying minimum pitch misalignments in case of strong turbulence, confirming the robustness of the approach with a different set of signals, shedding light to the capabilities of the method of reducing energy loss enabling early misalignment detection even in a less-than- ideal signals conditions. Furthermore, the adaptability of our classifier, relying on an Azimuth-based Fourier Transform, extends its applicability to simulations across varying wind speeds. Indeed, it assesses high detection performance and robustness regardless of wind speed variations in the considered velocity range, thus enhancing the versatility and practicality of our approach.

To provide further insights into the classification outcomes, Figure 3 provides a graphical representation of these results, showing the actual and the estimated severity degree for each predicted window. In the plot, each point represents a window, and its coordinates are the normalized area under the 1 $\times$ Rev harmonics for the Accelerations along Y and Z. As demonstrated in the Figure, the data are accurately classified. Indeed, predicted points consistently overlap with actual ones, indicating a strong correspondence between the real and predicted system behavior, although there is more overlap in the transition regions when considering features extracted from acceleration signals.

Given these results, the same approach is applied when considering a different set of features to test the performance of the approach: the peak amplitude of the 1 $\times$ Rev harmonics is considered. By considering F1-Score as a metric, our approach proved to be more effective at

Classification Report				
Label	**Precision**	**Recall**	**F1-score**	**Support**
Healthy	0.89	0.97	0.92	88
Low	0.85	0.83	0.88	121
Medium	0.92	0.93	0.93	210
High	0.99	0.6	0.76	37

Table 2. Metrics computed from the fault and quantification output considering spectra peak features

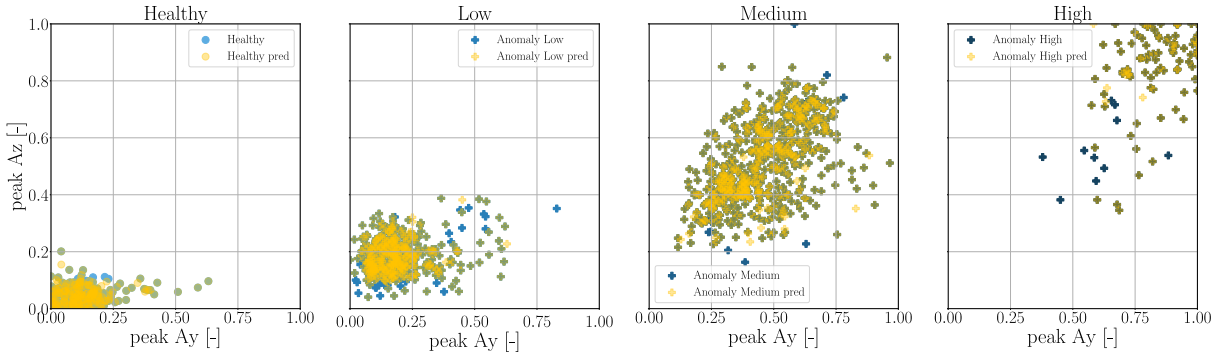

Figure 4. Misalignment Severity Assessment Results. This Figure shows a comparison of predicted misalignment severity (in yellow) with the actual one, considering the spectra peak as features, demonstrating consistency across severity levels

detecting the presence of misalignment and further classifying its severity class, with an average F1-Score of 90.1% regardless of the turbulence intensity and with a wind speed ranging again from 11 to 25 m/s. All the other metrics, showing an increase of performance for each class are reported in Table 2.

Again, Figure 4 provides a graphical representation of these results. In the plot, each point represents again a window, and its coordinates are the normalized amplitude of the peak of the $1 \times$ Rev harmonics for the lateral and top-down Accelerations. As demonstrated in the figure, the data are still accurately classified, as predicted points consistently overlap with actual ones.

Once misalignment detection is completed, the following step is to localize the misaligned blades. Figure 5 illustrates a comparison between the true condition and predictions made by the second layer random forest classifier. Instances are reported in a two-dimensional feature space, with

Classification Report				
Label	**Precision**	**Recall**	**F1-score**	**Support**
Blade 1 +	0.97	0.97	0.97	32
Blade 1 -	1.0	0.97	0.98	32
Blade 2 +	0.76	1.00	0.86	16
Blade 2 -	0.82	0.88	0.85	16
Blade 3 +	0.93	0.81	0.87	16
Blade 3 -	1.00	0.81	0.90	16

Table 3. Metrics computed from the fault localization algorithm

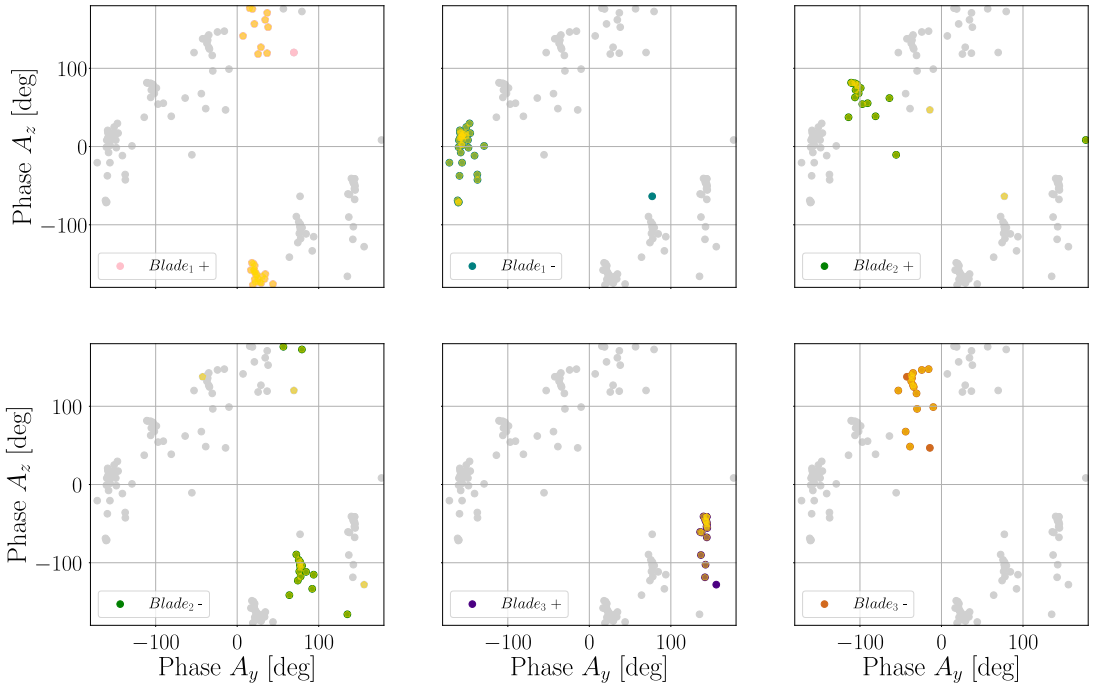

Figure 5. In this figure the accelerations 1 × Rev harmonics phases are reported in colors and the predicted instances are reported in yellow. As demonstrated in the figure, the data are still accurately classified, as predicted points consistently overlap with actual ones for each misaligned blade and for each sign of misalignment. The whole dataset is shown in gray.

.

each point representing the phase value of the 1 × Rev harmonics for Accelerations along y and z axis. These results prove the effectiveness of our approach in accurately localizing the misaligned blades. Additionally, Table 3 provides a quantitative overview of these results, presenting metrics computed for the second classification phase. Specifically, the average F1-score assessed by the model is 95.3%.

6. Conclusions

In this work, we build upon our previously developed method machine-learning framework specifically tailored for detecting pitch misalignment in wind turbines, considering a more affordable and readily available set of signals, i.e., those provided by the accelerometers on the fixed reference frame, as the only data source. Our goal was to analyze the signals and identify a set of effective features that would enable us to achieve performance comparable to that obtained using moment signals, which are generally more precise and less noisy. Considering the presented results, the proposed approach proves robustness in turbulent wind scenarios and different wind speeds, while preserving its inherent interpretability. This has been achieved by following an ad-hoc design of features that are related to the physical behaviour of the system. More in detail, our strategy extracts frequency domain features encompassing not only the area subtended under the peak at the 1 × Rev harmonics but also the amplitude of the peak itself, which are essential indicators for detecting the presence of rotor imbalances. In addition, to introduce the localization of the anomaly, relying solely on signals measured on the fixed reference frame, the phase of the 1 × Rev harmonics of accelerations signals has been introduced as a

feature. Validation of this approach through numerous experimental simulations featuring turbulent wind conditions, different wind speeds and pitch misalignment degree allowed us to asses the performance of the method in detecting and localizing the anomaly considering a scenario that perfectly resembles actual operating conditions of the wind turbines. More specifically, the method yields an average F1-score up to 90.1% in detection of the anomaly ranging from a pitch misalignment from 0.5 to 2.0 degree on a single blade while it achieves an average F1-score of 95.3% in the localization of these anomalies. Going forward, our research will concentrate on several directions: broadening the range of wind velocities to assess detection performance even at low wind speeds, and examining additional causes of rotor imbalance, including mass imbalances and ice accretion on the blades. This evolution aims to provide a more comprehensive and precise fault diagnosis, considering that these faults indeed can exhibits the same symptoms in the frequency behaviour of the system. Such advancements would contribute to the transition from a time-based to a condition-based turbine maintenance scheduling approach, ultimately reducing downtime and optimizing energy production.

References

[1] Per B, Søren D and Morgens B 2011 Diagnosis of pitch and load effects international Patent Classification

[2] Cacciola S, Munduate Agud I and Bottasso C L 2016 Detection of rotor imbalance, including root cause, severity and location *Journal of Physics: Conference Series* vol 753 p 072003

[3] Sha D, Li Q, Zou X and Zhu M 2021 Wind turbine variable pitch system fault monitoring method and system huaneng Clean Energy Research Institute

[4] Cacciola S, Riboldi C E D and Croce A 2018 Monitoring rotor aerodynamic and mass imbalances through a self-balancing control *Journal of Physics: Conference Series* vol 1037 p 032041

[5] Bertelè M, Bottasso C L and Cacciola S 2018 Automatic detection and correction of pitch misalignment in wind turbine rotors *Wind Energy Science* **3** 791–803

[6] Cacciola S and Riboldi C E D 2017 Equalizing aerodynamic blade loads through individual pitch control via multiblade multilag transformation *Journal of Solar Energy Engineering* **139** 061008

[7] Kusiak A and Verma A 2011 A data-driven approach for monitoring blade pitch faults in wind turbines *IEEE Transactions on Sustainable Energy* **2** 87–96

[8] Milani S, Leoni J, Cacciola S, Croce A and Tanelli M 2024 Automatic detection and intensity classification of pitch misalignment of wind turbine blades: a learning-based approach *Journal of Physics: Conference Series* vol 2767 (IOP Publishing) p 032010 URL `https://dx.doi.org/10.1088/1742-6596/2767/3/032010`

[9] Milani S, Leoni J, Cacciola S, Croce A and Tanelli M 2025 A machine-learning-based approach for active monitoring of blade pitch misalignment in wind turbines *Wind Energy Science* **10** 497–510 URL `https://wes.copernicus.org/articles/10/497/2025/`

[10] Jonkman J, Butterfield S, Musial W and Scott G 2009 Definition of a 5-mw reference wind turbine for offshore system development Tech. rep. NREL URL `https://www.osti.gov/biblio/94742`

[11] Bottasso C L and Croce A 2009–2018 *Cp-Lambda user manual* Dipartimento di Scienze e Tecnologie Aerospaziali, Politecnico di Milano Milano, Italy

[12] Garrad Hassan and Partners Ltd 2004 *IEC 61400-1 Ed.3. Wind Turbines — Part 1: Design requirements*

[13] Breiman L 2001 Random forests *Machine Learning* **45** 5–32

[14] Ceriani L and Verme P 2012 The origins of the gini index: extracts from variabilità e mutabilità (1912) by corrado gini *The Journal of Economic Inequality* **10** 421–443